Synthesis and molecular structures of palladium and platinum complexes of PTFA: models of Grignard cross-coupling catalysts

Brigitte Jedlicka [a], Richard E. Rülke [a,1], Walter Weissensteiner [a,*], Rafael Fernández-Galán [b], Félix A. Jalón [b], Blanca R. Manzano [b,*], Jerónimo Rodríguez-de la Fuente [b], Nora Veldman [c], Huub Kooijman [c], Anthony L. Spek [c,2]

[a] *Institut für Organische Chemie der Universität Wien, Währingerstraße 38, A-1090 Wien, Austria*

[b] *Departamento de Química Inorgánica, Orgánica y Bioquímica, Universidad de Castilla-La Mancha, Campus Universitario, 13071 Ciudad Real, Spain*

[c] *Bijvoet Center of Biomolecular Research, Vakgroep Kristal- en Structuurchemie, Utrecht University, Padualaan 8, 3584 CH Utrecht, Netherlands*

Abstract

A number of palladium(0) and palladium(II) as well as platinum(0) and platinum(II) complexes of (η^5-cyclopentadienyl)-(η^5-4-*endo*-N,N-dimethylamino-3-diphenylphosphino-4,5,6,7-tetrahydro-1H-indenyl)iron (PTFA) of the type (PTFA)M(0)(alkene) and (PTFA)M(II)(R)X, (M = Pd, Pt; alkene = dibenzylideneacetone, maleic anhydride, fumaronitrile and tetracyanoethylene; R = CH$_3$, Ph and PhCH$_2$; X = Cl, Br and I) have been synthesized as models of Grignard cross-coupling catalysts. All complexes were prepared either by proper ligand exchange or via oxidative addition reactions. A comparison of the X-ray structures of five complexes ((PTFA)Pd(fumaronitrile), **4**, (PTFA)PdCl$_2$, **8**, (PTFA)Pd(Ph)I, **10**, (PTFA)Pt(tetracyanoethylene), **6**, and (PTFA)Pt(CH$_3$)Cl, **13**) showed that, in contrast to complexes of 2-(1-N,N-dimethylaminoethyl)-1-diphenylphosphino-ferrocene (PPFA), the overall molecular structures of PTFA complexes are comparable; they neither strongly depend on the oxidation state of the metal nor on the type of additional ligands coordinated to the metal. Compound **4**, C$_{32}$H$_{32}$FeN$_3$PPd · CH$_2$Cl$_2$, crystallizes in the monoclinic space group $P2_1/c$ (no. 14), with $a = 19.237(2)$, $b = 9.0737(10)$, $c = 17.917(3)$ Å, $\beta = 96.458(11)°$, $V = 3107.6(7)$ Å^3, $Z = 4$. The structure refinement converged to $R1 = 0.0579$ for 3832 $F_0 > 4\sigma(F_0)$ and $wR2 = 0.1276$ for all 6520 unique data, $S = 0.94$. Compound **6**, C$_{34}$H$_{30}$FeN$_5$PPt · C$_4$H$_{10}$O, crystallizes in the triclinic space group $P\bar{1}$ (no. 2), with $a = 11.845(3)$, $b = 12.120(4)$, $c = 12.979(3)$ Å, $\alpha = 81.68(2)°$, $\beta = 82.06(2)°$, $\gamma = 68.11(3)°$, $V = 1703.6(8)$ Å^3, $Z = 2$. The structure refinement converged to $R1 = 0.0402$ for 6459 $F_0 > 4\sigma(F_0)$ and $wR2 = 0.1076$ for all 7235 unique data, $S = 1.04$. Compound **13**, C$_{29}$H$_{33}$ClFeNPPt, crystallizes in the monoclinic space group $P2_1/c$ (no. 14), with $a = 16.122(2)$, $b = 10.1608(11)$, $c = 21.716(3)$ Å, $\beta = 132.202(11)°$, $V = 2635.2(5)$ Å^3, $Z = 4$. The structure refinement converged to $R1 = 0.0322$ for 3846 $F_0 > 4\sigma(F_0)$ and $wR2 = 0.0734$ for all 4612 unique data, $S = 1.03$.

1. Introduction

A number of ferrocenyl phosphines have been used successfully as ligands for enantioselective homogeneous catalysts [1,2]. Most of these ligands are derivatives of 2-(1-N,N-dimethylaminoethyl)-1-diphenylphosphino-ferrocene, PPFA (**1**, Scheme 1), which in a variety of carbon–carbon bond-forming reactions has given high chemical and optical yields (> 95%) [1,2]. However, despite their unquestioned success the enantioselectivity introduced by these ligands is highly dependent on a number of parameters, e.g. on their substitution pattern or on structural changes of the substrates used. Hence, ligand development is still an active and ongoing field, especially directed towards the design of catalysts applicable to a broader range of reactions and substrates [3].

Recently, we have reported on aminoalcohol and aminophosphine derivatives of α-dimethylamino-1,2-tetramethylene-ferrocene and their use in the alkylation of aldehydes and Grignard cross-coupling reactions [4–8]. While alkylations of aldehydes with diethyl zinc gave

---

* Corresponding authors.
[1] On leave of absence from the University of Amsterdam.
[2] Corresponding author pertaining to the crystallographic study.

excellent optical yields (up to 93%), the enantioselectivity in the Grignard cross-coupling as exemplified by reaction of phenethyl magnesium chloride with vinyl bromide to give 3-phenyl butene as the final product reached 79% e.e. An enormous dependence of the enatioselectivity on the three-dimensional structure of the ligands was observed. Optical yields of 79% were found with the dichloropalladium complex of (η^5-cyclopentadienyl)-(η^5-4-endo-N,N-dimethylamino-3-diphenylphosphino-4,5,6,7-tetrahydro-1H-indenyl)iron (PTFA), (R)-(R$_m$)-2 (2a), as the catalyst precursor, but the enantioselectivity dropped to 4% e.e. when the diastereomer with the opposite configuration at the benzylic carbon, (S)-(R$_m$)-2 (2b), was used (Scheme 1). These results are in contrast to those reported previously from the dichloropalladium complex of (S)-(R$_m$)-PPFA, (1), and its diastereomer (R)-(R$_m$)-PPFA which gave optical yields in that particular cross-coupling reaction of 68% e.e. and 54% e.e. respectively [9].

In a recent conformational study of palladium–PPFA complexes we have shown that such complexes are highly flexible and can adopt several different conformations in the solid state, depending on the additional ligands and on the oxidation state of the metal [10]. Since it is expected that ligands 2a and 2b have less conformational flexibility, we were interested in the molecular structures of complexes of 2a, especially of those expected to be intermediates in the catalytic system of enantioselective Grignard cross-coupling reactions (Scheme 2). According to a proposal of Hayashi et al. [11] and an NMR study of Brown and coworkers [12,13], the catalyst precursor, usually a palladium(II) complex, is reduced to a palladium(0) species which subsequently oxidatively adds vinyl bromide. To this palladium(II) intermediate the alkyl group of the Grignard reagent is transferred. Subsequent reductive elimination leads to the final product regenerating the original palladium(0) species.

We now describe the synthesis and structural analysis of a number of palladium and platinum complexes of 2a which are expected to be intermediates or can serve as models for such intermediates in catalytic Grignard cross-coupling reactions.

2. Synthesis and structural characterization

Palladium(0) and platinum(0) complexes 4, 5 and 7 were prepared in fairly high yields (88%, 70% and 59% respectively) by reaction of ligand 2a (N–P) with Pd$_2$(dba)$_3$(CHCl$_3$) or Pt$_2$(dba)$_3$(CHCl$_3$) [14] (dba = dibenzylideneacetone) and fumaronitrile (4), or maleic anhydride (5, 7) according to Scheme 3 (i). When the reaction with the palladium precursor is carried out in the absence of olefin or with less electron-accepting olefins such as acrylonitrile or methyl acrylate, the

complex (PTFA)Pd(dba), 3, is obtained. The tetracyanoethylene platinum(0) complex 6, as well as the palladium(II) and platinum(II) complexes 8–13 are accessible via ligand substitution reactions (6 in 26% yield (Scheme 3 (ii)) [15] and 9–13 in yields greater than 90% (Scheme 3, (iii)–(vi)). Cyclooctadiene palladium and platinum precursors (COD)M(R)X [16,17] were used to synthesize complexes 9, 12, and 13, while substitution of bisnitrogen ligands tetramethylethylenediamine (TMEDA) or bipyridine (bipy) [18,19] gave access to 10 and 11, respectively. The synthesis of the dichloropalladium complex 8 was achieved by reaction of 2a with dichloro(bisacetonitrilo)palladium(II) [4]. Complex 10 could also be obtained via oxidative addition (Scheme 3 (vii)). When this reaction is carried out with bromides RBr (R = Ph, PhCH$_2$, CH=CH$_2$), in each case a mixture of the desired product and the dibromide complex is obtained. In the case of the (PTFA)Pd(CH=CH$_2$)Br complex, an increasing amount of dibromide is observed when the evolution of the mixture is monitored by ^{1}H-NMR. Therefore, it is reasonable to assume a disproportionation process to be responsible for the formation of the observed dibromide derivatives.

(S)-(R$_m$)-1   (R)-(R$_m$)-2a   (S)-(R$_m$)-2b
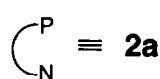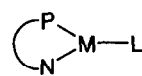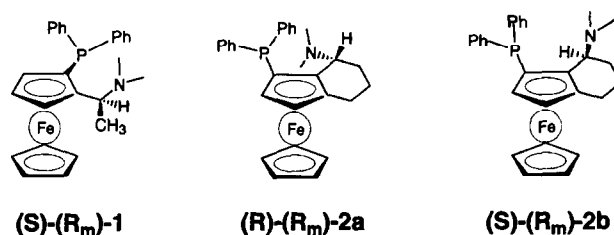
M	L	
Pd	dba	3
Pd	FN	4
Pd	MA	5
Pt	TCNE	6
Pt	MA	7
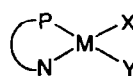
| M	X	Y	
Pd	Cl	Cl	8
Pd	CH$_3$	Cl	9
Pd	Ph	I	10
Pd	PhCH$_2$	Br	11
Pt	Cl	Cl	12
Pt	CH$_3$	Cl	13

Scheme 1.

It is evident from the ^{1}H, ^{13}C and ^{31}P NMR spectra that in each complex of 2a the amino phosphine acts as a bidentate ligand as judged, for example, from the inequivalence of the diastereotopic aminomethyl groups which are equivalent in 2a. On coordination, the resonance signals of these methyl groups appear at higher frequencies compared with the signal of the free ligand [5], a reasonable fact considering the donation of electron density from the nitrogen to the metal centre. Conversely, the alkene protons and carbons are shifted to lower frequency by 2.6–3.8 ppm (1.9–2.3 ppm for 3) in the ^{1}H-NMR and by about 90 ppm in the ^{13}C-NMR spectra. These chemical shifts are in the range usually observed for other zero valent ML$_2$(alkene) complexes of palladium and platinum [20–26]. As expected, the proton–proton coupling constant of the cis olefinic protons (J_{H-H} cis) of 5 is clearly smaller than that of the trans protons (J_{H-H} trans) of 4. The alkyl or aryl groups in complexes 9, 10, 11 and 13 are in a trans position to the coordinated nitrogen donor ligand as judged from the $^2J_{P-C}$ coupling constants (2.5–7 Hz) and confirmed via crystal structure analysis of 10 and 13 (see below). For vinyl palladium(II) complexes of PPFA, 1, Brown and coworkers reported P–C coupling constants for cis and trans P–Pd–C arrangements of 6
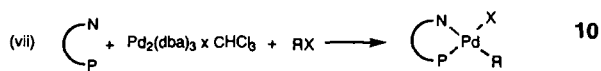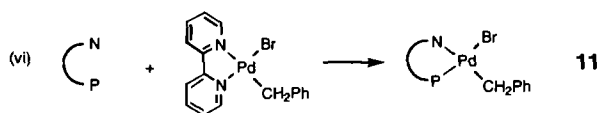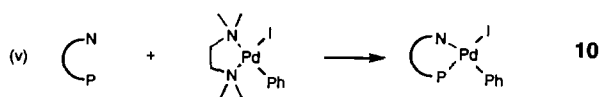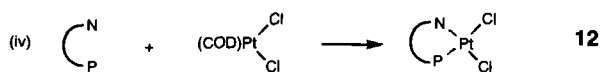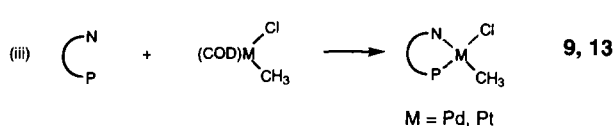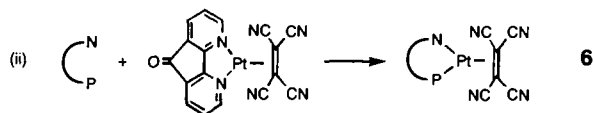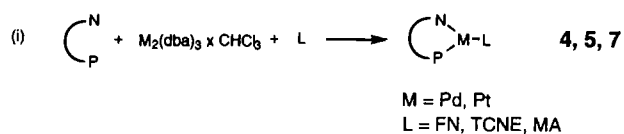
to 18 Hz and 96 to 128 Hz respectively [13]. This ligand substitution pattern is in agreement with the antisymbiotic behaviour of palladium [27,28]. As seen from the proton NMR spectrum, complex 3 is fluxional at room temperature in a C$_6$D$_6$ solution. Since either olefinic group of dba can coordinate to the (PTFA)Pd unit, several diastereomers are feasible. Interconversion of these diastereomers might explain the observed exchange process. The ^{1}H-NMR at room temperature shows four signals for the aminomethyl groups and single resonances for all other groups. All signals appear significantly broadened at ambient temperature. Complex 3 decomposes over a period of several hours on standing in solution (C$_6$D$_6$), probably due to the poor electron-accepting character of the olefin. This fact has prevented recording of a ^{13}C-NMR spectrum.

NMR analysis also showed that, in solution, the fumaronitrile and maleic anhydride complexes 4 and 5 are present as two diastereomers, while single isomers were formed in all other cases.

For the maleic anhydride complex 5 the ratio of diastereomers (rotamers) is strongly solvent dependent (70 : 30 in C$_6$D$_6$ and 55 : 45 in CDCl$_3$), indicating a fast isomer interconversion at ambient temperatures. Contrary to 5, the interconversion of diastereomers of the
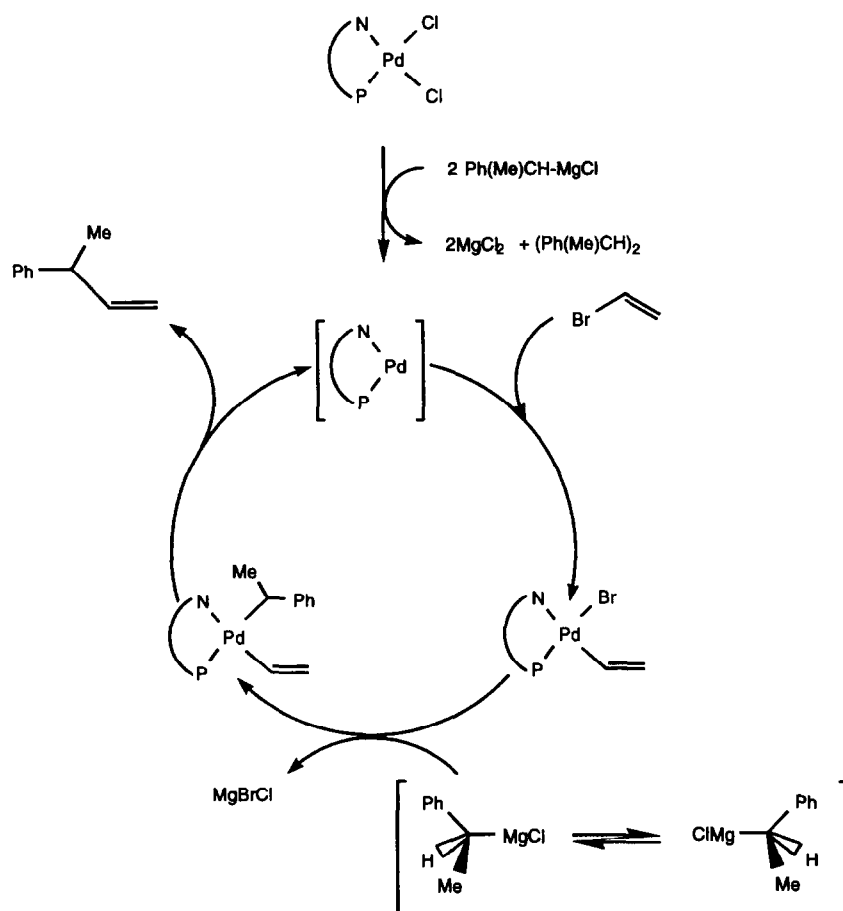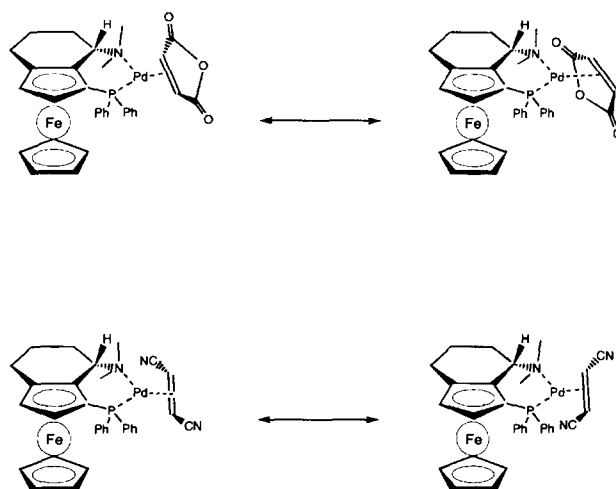

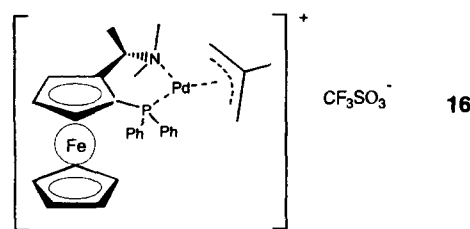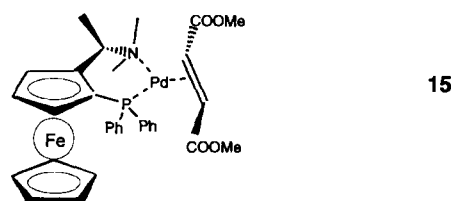Scheme 2. Proposed catalytic cycle of a palladium-induced Grignard cross-coupling reaction.

Scheme 3.

Scheme 4. Feasible interconversions of the diastereomers (rotamers) of 4 and 5.

fumaronitrile; however, other mechanisms not involving dissociation of the olefin cannot yet be excluded.

3. Molecular structures of complexes 4, 6, 10 and 13

As mentioned above, a comparison of the molecular structures of palladium PPFA complexes 14–16 (Scheme 5) showed that the PPFA ligand, even in the solid state, can adopt significantly different conformations, depending on the type of additional substituents at

fumaronitrile complex 4 could be studied quantitatively. Preparation of 4 under kinetic control (see Experimental) gave a sample in which one diastereomer was highly enriched (better than 9:1). The interconversion of both diastereomers was followed via proton NMR spectroscopy in benzene-d^6 as well as in chloroform-d^1. In both solvents an equilibrium ratio of 62:38 was finally reached, and similar rate constants were measured for these processes: $k = 1.3 \times 10^{-5}$ s^{-1} in C_6D_6 and 4.5×10^{-5} s^{-1} in CDCl$_3$. From these rate constants the interconversion barriers of the major isomer were calculated to be $\Delta G^{\ddagger}(298K) = 94 \pm 2$ kJ mol^{-1} and 97 ± 2 kJ mol^{-1}, respectively. While interconversion of diastereomers of 5 can, for example, be achieved via rotation of the maleic anhydride ligand along the palladium olefin bond, such a mechanism can be excluded for 4. In order to achieve isomerization of 4, the palladium has to change its coordination site at the fumaronitrile unit (Scheme 4). The most likely mechanism seems to be a dissociation–association sequence of

Scheme 5.

the square-planar palladium unit [10]. Whereas in the dichloropalladium complex **14** the palladium moiety including the dimethylamino nitrogen is found in an exo-position (Pd 1.38 Å above the substituted cyclopentadienyl ring, Cp¹), in **15** and **16** the palladium is found 0.17 Å and 0.05 Å respectively below that plane. Although the palladium is located below Cp¹ in both cases, the six-membered palladium chelate rings of **15** and **16** adopt different conformations with the dimethylamino nitrogen either below (0.56 Å, **15**) or above (0.29 Å, **16**) the cyclopentadienyl ring, placing the methyl group of the ethyl side chain in a pseudo-axial or pseudo-equatorial position respectively.

Since the side chain flexibility in ligand **2a** is significantly reduced compared with PPFA, a reduced conformational flexibility of the corresponding palladium or platinum complexes might also be expected. In the next paragraphs the molecular structures of complexes **4, 6, 10** and **13** are described and compared with that of the dichloropalladium complex **8** [4], an actual catalyst precursor of the enantioselective Grignard cross-coupling mentioned above.

All diffraction data were collected at low temperature (150 K). The structures were solved with direct methods and refined with least squares as described in the Experimental Section. Complexes **4** and **6** crystallize in the monoclinic group $P2_1/c$ with four symmetry-related molecules in the unit cell. Crystals of **13** belong to the triclinic space group $P\bar{1}$ with two symmetry-related molecules in the unit cell. The molecular structure of **10** could be solved in space group $P\bar{1}$ but owing to very poor crystal quality, refinement was only possible to a residual R of 17%. Hence, this structure can only be considered as preliminary and the analysis takes into account only some general structural features. The molecular structures of **4, 6, 8, 10** and **13** and the adopted numbering scheme are shown in Figs. 1–5, crystal data and final atomic coordinates are listed in Tables 1–4.

The general structural features of complexes **4, 6, 8** and **13**, especially those of the ferrocenyl part, are very similar. The cyclopentadienyl rings are essentially planar, adopting a slightly tilted arrangement with tilt angles ranging from 6.3(4)° (**6**) to 9.5(3)° (**8**). Bond lengths and bond angles in the ferrocene unit are normal, the average Fe–Cp bond lengths are 2.042(11), 2.043(9), 2.045(11) and 2.045(16) Å for **4, 6, 8** and **13** respectively, and the average C_{ar}–C_{ar} bond lengths are 1.415(21), 1.417(11), 1.416(10) and 1.413(16) Å respectively. In all cases the amino nitrogen adopts an endo-position with the C11–N1 bond pointing towards the proximal side of the substituted cyclopentadienyl ring (towards the iron-coordinated Cp side). The dimethylamino group in complexes **4, 8** and **13** adopts a pseudo-axial conformation, while a pseudo-equatorial conformation is found for **6**. In principle, both confor-

Fig. 1. An ORTEP [33] plot of **4** at 50% probability level; hydrogen atoms and solvent molecules were left out for clarity.

mations are interconvertible via an inversion of the six membered ring C2–C11–C12–C13–C14–C3. Such an inversion significantly changes the positions of carbons C12 and C13; in pseudo-axial conformations C12 is located on the distal and C13 on the proximal side of the Cp¹ ring, while in the pseudo-equatorial conformation an opposite arrangement is found (Table 5). The phosphorus atom is slightly displaced towards the distal side in complexes **6, 8** and **13**, but essentially in-plane with the Cp¹ ring in **4**. In all cases, including **10**, the limited conformational flexibility of the coordinating nitrogen N1 forces the square-planar palladium or platinum units onto the proximal Cp¹ side independently of the pseudo-axial or pseudo-equatorial conformation of the dimethylamino group.

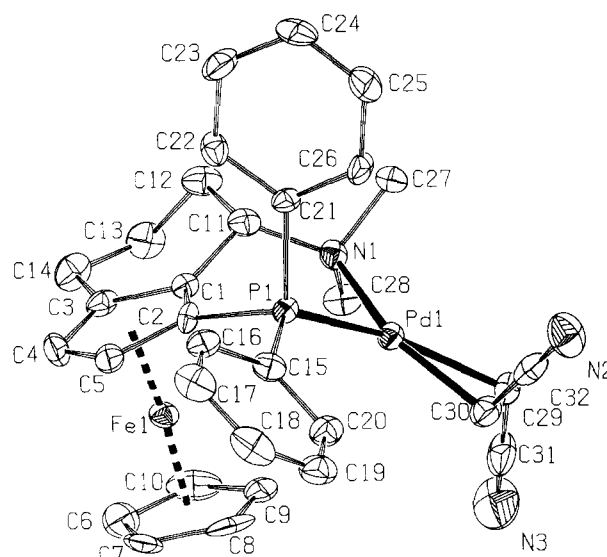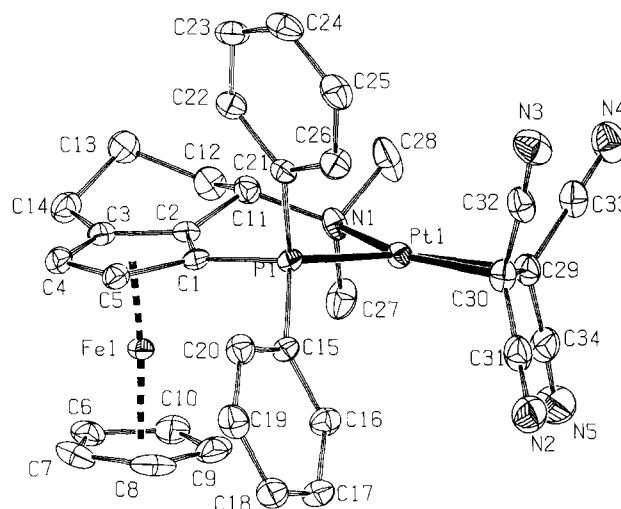

Fig. 2. An ORTEP [33] plot of **6** at 50% probability level; hydrogen atoms and solvent molecules were left out for clarity.
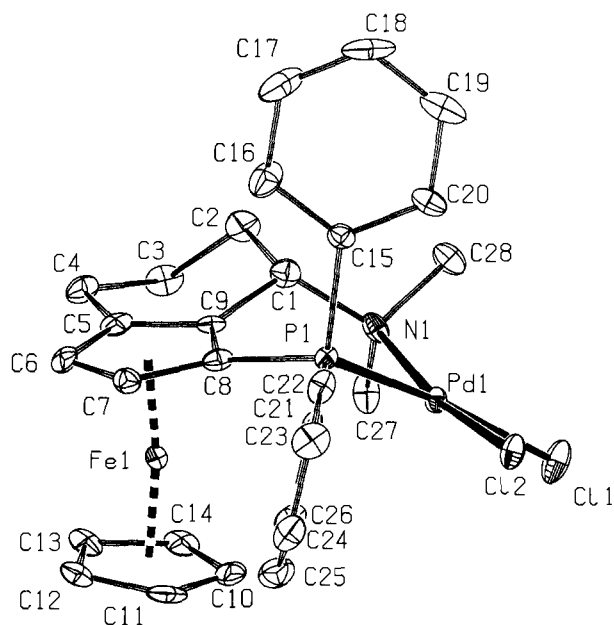
Fig. 3. An ORTEP [33] plot of **8** at 50% probability level; hydrogen atoms were left out for clarity.

Fig. 5. An ORTEP [33] plot of **13** at 50% probability level; hydrogen atoms were left out for clarity.

As a consequence of the different trans-influences of the amino nitrogen and the phosphino phosphorus, the aryl or alkyl groups of **10** and **13** are found in a position trans to the coordinating nitrogen donor atom. As expected, the Pd–Cl bond lengths differ significantly in **8**, the Pd–Cl bond trans to the phosphorus being 0.095 Å longer than the Pd–Cl bond trans to the nitrogen, again indicating the stronger trans-influence of phosphines compared with amines. A similar behaviour has been observed for the palladium(0) and platinum(0) complexes **4** and **6** in which the metal carbon bond trans to

Fig. 4. An ORTEP [33] plot of **10** at 50% probability level; hydrogen atoms were left out for clarity.

the phosphine is longer by 0.089 Å and by 0.110 Å respectively.

In all structures the palladium or platinum square-planar unit adopts a conformation which places one methyl group of the dimethylamino unit in a pseudo-equatorial (C27) and one in a pseudo-axial position (C28). In this conformation, the pseudo-axial group effectively blocks one side of the square-planar palladium or platinum unit, which may have a significant effect on the enantioselectivity of the catalytic reaction.

The crystal structure analysis of complexes **4, 6, 8, 10** and **13** clearly shows that conformational flexibility in complexes of PTFA is severely reduced compared with their PPFA analogues; in addition they do not depend significantly on the oxidation state or on the substitution pattern of the metal. From these results it might be expected that in (PTFA)Pd-catalyzed Grignard cross-coupling reactions the (PTFA)Pd unit retains its structural integrity during the several stages of the catalytic cycle.

4. Experimental

NMR spectra were run in $CDCl_3$ (unless otherwise stated) on Bruker AMX-300, AC-250 and on Varian Unity FT-300 spectrometers. ^{13}C-NMR spectra were run in a J-modulated mode. Chemical shifts, δ, are given relative to TMS (^1H-, ^{13}C-NMR) and 85% H_3PO_4 (^{31}P-NMR). Melting points were determined on a Kofler melting point apparatus and are uncorrected. Elemental analyses were partly carried out at Mikroanalytisches Laboratorium der Universität Wien (Mag. J. Theiner)

and partly with a Perkin-Elmer 2400 microanalyser. All reactions were carried out in an inert atmosphere using standard Schlenk techniques.

4.1. {[η⁵-Cyclopentadienyl]-[η⁵-4-(endo-N,N-dimethyl-amino)-3-(diphenylphosphino)-4,5,6,7-tetrahydro-1H-indenyl]-iron}(η²-dibenzylideneacetone)palladium(0), 3

To a degassed solution of $Pd_2(dba)_3(CHCl_3)$ (85.8 mg, 0.083 mmol) in 20 ml of toluene is added 93 mg (0.200 mmol) of 2a. The mixture is stirred for 3 h, filtered and evaporated to dryness. The residue is washed with hexane (3 × 10 ml) and the remaining brown solid is recrystallized from toluene–hexane.

Yield: 16.3 mg (12%). Anal. Found: C, 66.37; H, 5.55; N, 1.89. $C_{45}H_{44}FeNOPPd$. Calc.: C, 66.89; H, 5.49; N, 1.73%. ¹H-NMR: δ 0.72, 1.07, 1.37, 1.74, 1.95 (br, 6H, skeletal hydrogens), 2.55, 2.73, 2.92, 3.03 (br, N–CH₃), 3.66 (s, 1H, Fc), 3.79 (s, 5H, Fc), 3.96 (s, 1H, Fc), 4.88, 5.53 (br, olefinic hydrogens), 6.4–8.2 (m, 20H, Ph).

4.2. {[η⁵-Cyclopentadienyl]-[η⁵-4-(endo-N,N-dimethyl-amino)-3-(diphenylphosphino)-4,5,6,7-tetrahydro-1H-indenyl]-iron}(η²-fumaronitrile)palladium(0), 4

To a degassed solution of 18 mg (0.017 mmol) $Pd_2(dba)_3(CHCl_3)$ in 5 ml toluene a degassed solution of 18 mg (0.038 mmol) of 2a in toluene is added. After

Table 1
Crystallographic data for compound 4, 6 and 13

Compound	4	6	13
Crystal data			
Formula	$C_{32}H_{32}FeN_3PPd \cdot CH_2Cl_2$	$C_{34}H_{30}FeN_5PPt \cdot C_4H_{10}O$	$C_{29}H_{33}ClFeNPPt$
Molecular weight	736.80	864.67	712.93
Crystal system	monoclinic	triclinic	monoclinic
Space group	$P2_1/c$ (No. 14)	$P\bar{1}$ (No. 2)	$P2_1/c$ (No. 14)
a (Å)	19.237(2)	11.845(3)	16.122(2)
b (Å)	9.0737(10)	12.120(4)	10.1608(11)
c (Å)	17.917(3)	12.979(3)	21.716(3)
α (deg)	90.00	81.68(2)	90.00
β (deg)	96.458(11)	82.06(2)	132.202(11)
γ (deg)	90.00	68.11(3)	90.00
V (Å³)	3107.6(7)	1703.6(8)	2635.2(5)
D_{calc} (g cm⁻³)	1.575	1.686	1.797
Z	4	2	4
F(000)	1496	860	1400
μ(cm⁻¹)(Mo K α)	13.0	46.1	60.3
Crystal size (mm³)	0.08 × 0.15 × 0.50	0.15 × 0.25 × 0.63	0.10 × 0.25 × 0.40
Data collection			
T (K)	150	150	150
θ_{SET4} − range	11.5–13.9	11.4–13.8	10.18–13.97
θ_{min}, θ_{max} (deg)	1.1, 27.5	1.6, 27.5	1.27, 25.0
Wavelength (Å) (graphite monochromator)	0.71073	0.71073	0.71073
Scan type	ω/2θ	ω/2θ	ω/2θ
X-ray exposure time (h)	16.0	20.4	10.6
Reference reflection	$60\bar{2}$, $32\bar{1}$, $20\bar{4}$	$20\bar{5}$, $\bar{1}2\bar{4}$, $44\bar{2}$	$20\bar{2}$, $0\bar{2}6$, $25\bar{4}$
Data set	−23:24, 0:11,−22:0	−14:14,−15:15,−16:0	−19:19,−1:12,−19:25
Total data	7180	7560	5124
Total unique data	6520	7235	4612
DIFABS correction range	0.714–1.387	0.601–1.716	0.632–1.369
Refinement			
No. of refined parameters	351	428	310
Final R1 [a] [no. of data]	0.0579 [3832 $F_0 > 4\sigma(F_0)$]	0.0402 [6459 $F_0 > 4\sigma(F_0)$]	0.0322 [3846 $F_0 > 4\sigma(F_0)$]
Final wR2 [b] [no. of data]	0.1276 [6520]	0.1076 [7235]	0.0734 [4612]
S	0.94	1.04	1.03
w [c]	$\sigma^2(F^2) + (0.0512P)^2$	$\sigma^2(F^2) + (0.0828P)^2 + 0.0744P$	$\sigma^2(F^2) + (0.0395P)^2$
$(\Delta/\sigma)_{av}$, $(\Delta/\sigma)_{max}$	0.000, 0.000	0.000, 0.001	0.001, 0.07
Min. and max. residual density (e Å⁻³)	−0.58, 0.73	−2.77, 3.24 (near Pt)	−1.54, 0.76 (near Pt)

[a] $R1 = \Sigma \| F_0 | - | F_c \| / \Sigma | F_0 |$; [b] $wR2 = [\Sigma[w(F_0^2 - F_c^2)^2]/\Sigma[w(F_0^2)^2]]^{1/2}$; [c] $P = (Max(F_0^2, '0) + 2F_c^2)/3$.

stirring for 5 min, 4 mg (0.05 mmol) of fumaronitrile is added and after an additional 30 min the solvent is removed in vacuo. The remaining precipitate is dissolved in 1 ml CH_2Cl_2, filtered off celite and precipitated by addition of diethyl ether, yielding 20 mg (0.031 mmol, 88%) of isomer A, which isomerizes in $CDCl_3$ to give an equilibrium mixture of A : B = 7 : 3. Crystals of isomer A suitable for X-ray analysis were obtained from CH_2Cl_2–hexane.

Anal. Found: C, 59.00; H, 5.01; N, 6.31. $C_{32}H_{32}FeN_3PPd$. Calc.: C, 58.98; H, 4.91; N, 6.45%.

Isomer A: ^{1}H-NMR: δ 1.53 (m, 1H), 1.69 (m, 1H), 1.93 (m, 1H), 2.05 (m, 1H), 2.28 (ddd, J = 5 Hz, 8 Hz, 16 Hz, 1H), 2.56 (m, 1H), 2.56 (dd, J = 9 Hz, 9 Hz, 1H, FN), 3.03 (s, 3H, N–CH_3), 3.30 (dd, J = 5 Hz, 7 Hz, 1H), 3.34 (s, 1H, N–CH_3), 3.48 (dd, J = 3 Hz, 9 Hz, 1H, FN), 3.94 (dd, J = 2 Hz, 2 Hz, 1H, Fc), 4.00 (s, 5H, Fc), 4.51 (d, J = 2 Hz, 1H, Fc), 7.2–7.8 (m, 10H, Ph). ^{13}C-NMR: δ 20.24, 22.21, 24.45 (d, J = 12 Hz, FN), 24.93 (d, J = 2.5 Hz, FN), 25.34, 43.35 (N–CH_3), 52.02 (N–CH_3), 60.62 (d, J = 2 Hz), 66.63 (d, J = 40 Hz, Fc), 69.06 (d, J = 1 Hz), 69.46, 69.78 (d, J = 3 Hz), 71.47 (Fc), 89.98 (d, J = 22 Hz, Fc), 91.36 (d, J = 8 Hz, Fc), 122.42 (d, J = 3 Hz, CN), 123.72 (d, J = 8 Hz, CN), 128.44 (d, J = 10 Hz, Ph), 128.64 (Ph), 129.35 (d, J = 2 Hz, Ph), 130.67 (d, J = 2.5 Hz, Ph), 131.94 (d, J = 14 Hz, Ph), 133.78 (Ph), 134.39 (d, J = 16 Hz, Ph), 135.10 (d, J = 34 Hz, Ph). ^{31}P-NMR: δ 13.92.

Isomer B: ^{1}H-NMR: δ 1.53 (m, 1H), 1.69 (m, 1H), 1.93 (m, 1H), 2.05 (m, 1H), 2.28 (m, 1H), 2.55 (m, 1H), 2.61 (dd, J = 9 Hz, 9 Hz, 1H, FN), 3.02 (s, 3H, N–CH_3), 3.20 (dd, J = 4 Hz, 9Hz, 1H, FN), 3.36 (s, 1H, N–CH_3), 3.98 (dd, J = 2 Hz, 2 Hz, 1H, Fc), 4.02

Table 2
Final coordinates and equivalent isotropic thermal parameters of the non-hydrogen atoms for compound **4**, $C_{32}H_{32}FeN_3PPd(CH_2Cl_2)$ (esds in parentheses)

Atom	x	y	z	$U(eq)(Å^2)$
Pd(1)	0.23110(2)	0.20147(6)	0.00089(2)	0.0193(1)
Fe(1)	0.15732(5)	−0.02708(10)	0.15576(5)	0.0203(3)
P(1)	0.29020(7)	0.1969(2)	0.11796(8)	0.0170(4)
N(1)	0.1375(2)	0.3179(6)	0.0372(3)	0.0209(16)
N(2)	0.3936(3)	0.2771(7)	−0.0965(3)	0.042(2)
N(3)	0.1246(4)	−0.0223(9)	−0.1637(4)	0.060(3)
C(1)	0.2269(3)	0.1423(7)	0.1792(3)	0.0175(17)
C(2)	0.1573(3)	0.1983(7)	0.1657(3)	0.0173(17)
C(3)	0.1173(3)	0.1335(7)	0.2208(3)	0.0222(17)
C(4)	0.1621(3)	0.0330(7)	0.2652(3)	0.027(2)
C(5)	0.2295(3)	0.0392(7)	0.2402(3)	0.0222(17)
C(6)	0.1003(4)	−0.2174(8)	0.1505(4)	0.041(3)
C(7)	0.1703(4)	−0.2479(7)	0.1497(4)	0.033(2)
C(8)	0.1938(4)	−0.1802(7)	0.0859(4)	0.038(2)
C(9)	0.1367(4)	−0.1061(7)	0.0484(4)	0.035(2)
C(10)	0.0795(4)	−0.1263(8)	0.0878(5)	0.044(3)
C(11)	0.1330(3)	0.3320(7)	0.1207(3)	0.0223(19)
C(12)	0.0621(3)	0.3851(8)	0.1422(4)	0.032(2)
C(13)	0.0128(3)	0.2631(8)	0.1614(4)	0.033(2)
C(14)	0.0436(3)	0.1765(8)	0.2285(4)	0.033(2)
C(15)	0.3683(3)	0.0919(7)	0.1462(3)	0.0231(17)
C(16)	0.4021(3)	0.1003(7)	0.2196(3)	0.028(2)
C(17)	0.4646(3)	0.0294(8)	0.2388(4)	0.035(2)
C(18)	0.4956(3)	−0.0503(8)	0.1859(4)	0.036(2)
C(19)	0.4639(3)	−0.0593(7)	0.1136(4)	0.031(2)
C(20)	0.4006(3)	0.0097(7)	0.0935(4)	0.0262(19)
C(21)	0.3166(3)	0.3816(7)	0.1513(3)	0.0191(17)
C(22)	0.3026(3)	0.4353(7)	0.2203(3)	0.0249(19)
C(23)	0.3246(4)	0.5774(8)	0.2417(4)	0.033(2)
C(24)	0.3605(4)	0.6627(7)	0.1949(4)	0.033(2)
C(25)	0.3751(4)	0.6066(8)	0.1287(4)	0.039(3)
C(26)	0.3543(4)	0.4656(7)	0.1067(4)	0.031(2)
C(27)	0.0744(3)	0.2480(7)	−0.0023(3)	0.029(2)
C(28)	0.1449(4)	0.4690(7)	0.0060(3)	0.0279(19)
C(29)	0.2184(4)	0.1677(7)	−0.1165(3)	0.026(2)
C(30)	0.2856(4)	0.1180(8)	−0.0796(3)	0.027(2)
C(31)	0.1671(4)	0.0593(9)	−0.1432(3)	0.036(2)
C(32)	0.3456(3)	0.2064(8)	−0.0894(3)	0.0277(19)

U(eq) is $1/3$ of the trace of the orthogonalized U.

(s, 5H, Fc), 4.48 (d, $J = 2$ Hz, 1H, Fc), 7.2–7.8 (m, 10H, Ph). ^{13}C-NMR: δ 20.13, 22.29, 24.70 (d, $J = 43$ Hz, FN), 25.06 (d, $J = 2.5$ Hz, FN), 25.21, 44.71 (N–CH_3), 51.78 (N–CH_3), 60.00 (d, $J = 1.5$ Hz), 71.47 (Fc), 128.36 (d, $J = 11$ Hz, Ph), 129.40 (d, $J = 1.5$ Hz, Ph), 130.59 (d, $J = 2$ Hz, Ph), 132.14 (d, $J = 15$ Hz, Ph), 143.44 (d, $J = 15$ Hz, Ph).

4.3. {[η^5-Cyclopentadienyl]-[η^5-4-(endo-N,N-dimethyl-amino)-3-(diphenylphosphino)-4,5,6,7-tetrahydro-1H-indenyl]-iron}(η^2-maleic anhydride)palladium(0), 5

The procedure is identical to that described for **4**, except that 5 mg (0.05 mmol) of maleic anhydride is used. The product consists of a mixture of the two

Table 3

Final coordinates and equivalent isotropic thermal parameters of the non-hydrogen atoms for compound **6**, $C_{34}H_{30}FeN_5PPt(C_4H_{10}O)$ (esds in parentheses)

Atom	x	y	z	U(eq) (Å^2)
Pt(1)	0.26454(2)	0.15582(2)	0.87973(1)	0.0181(1)
Fe(1)	0.21102(6)	−0.10603(6)	0.69273(5)	0.0173(2)
P(1)	0.33754(11)	0.10270(11)	0.71905(9)	0.0156(3)
N(1)	0.2745(4)	−0.0183(4)	0.9543(3)	0.0217(12)
N(2)	0.0737(6)	0.4967(5)	0.7707(4)	0.0400(17)
N(3)	0.4397(5)	0.3612(5)	0.8728(4)	0.0359(17)
N(4)	0.3076(6)	0.2696(5)	1.1461(4)	0.0390(19)
N(5)	−0.0441(5)	0.3317(6)	1.0284(5)	0.0457(19)
C(1)	0.3455(4)	−0.0431(4)	0.7046(4)	0.0160(12)
C(2)	0.3445(4)	−0.1329(4)	0.7892(4)	0.0163(12)
C(3)	0.3632(5)	−0.2405(5)	0.7455(4)	0.0197(12)
C(4)	0.3776(5)	−0.2180(5)	0.6351(4)	0.0230(17)
C(5)	0.3662(5)	−0.0976(5)	0.6092(4)	0.0202(14)
C(6)	0.0780(5)	−0.1767(5)	0.6929(5)	0.0275(17)
C(7)	0.0938(6)	−0.1146(6)	0.5956(5)	0.0324(19)
C(8)	0.0700(5)	0.0054(6)	0.6117(5)	0.0348(17)
C(9)	0.0394(5)	0.0168(6)	0.7196(5)	0.0329(19)
C(10)	0.0446(5)	−0.0966(6)	0.7698(5)	0.0297(17)
C(11)	0.3517(5)	−0.1336(5)	0.9052(4)	0.0214(14)
C(12)	0.3308(6)	−0.2443(5)	0.9647(4)	0.0276(17)
C(13)	0.4125(6)	−0.3571(5)	0.9148(5)	0.0296(17)
C(14)	0.3715(5)	−0.3568(5)	0.8094(4)	0.0269(17)
C(15)	0.2519(5)	0.1990(4)	0.6148(4)	0.0186(12)
C(16)	0.1278(5)	0.2635(5)	0.6365(4)	0.0243(17)
C(17)	0.0561(5)	0.3314(5)	0.5572(5)	0.0292(17)
C(18)	0.1090(6)	0.3355(5)	0.4556(5)	0.0313(17)
C(19)	0.2315(6)	0.2730(5)	0.4334(4)	0.0279(16)
C(20)	0.3034(5)	0.2050(5)	0.5126(4)	0.0234(16)
C(21)	0.4934(5)	0.0964(5)	0.6884(4)	0.0177(12)
C(22)	0.5910(5)	−0.0129(5)	0.6978(4)	0.0221(16)
C(23)	0.7106(5)	−0.0167(6)	0.6837(4)	0.0269(17)
C(24)	0.7334(5)	0.0882(6)	0.6604(4)	0.0291(18)
C(25)	0.6373(6)	0.1972(6)	0.6509(5)	0.0297(17)
C(26)	0.5187(5)	0.2012(5)	0.6645(4)	0.0267(17)
C(27)	0.1447(6)	−0.0080(6)	0.9763(5)	0.0331(17)
C(28)	0.3241(8)	−0.0254(6)	1.0559(5)	0.041(2)
C(29)	0.1866(5)	0.2862(5)	0.9900(4)	0.0235(16)
C(30)	0.2321(5)	0.3325(5)	0.8827(4)	0.0256(17)
C(31)	0.1425(6)	0.4249(5)	0.8202(4)	0.0290(16)
C(32)	0.3464(6)	0.3516(5)	0.8779(4)	0.0269(17)
C(33)	0.2536(6)	0.2784(5)	1.0771(4)	0.0267(16)
C(34)	0.0577(6)	0.3148(5)	1.0119(4)	0.0301(16)
O(1)	0.2558(4)	0.5638(4)	0.3744(3)	0.0361(14)
C(35)	0.2849(7)	0.5255(7)	0.5531(6)	0.45(2)
C(36)	0.3457(6)	0.5035(6)	0.4450(6)	0.0410(19)
C(37)	0.3006(7)	0.5409(7)	0.2687(6)	0.045(2)
C(38)	0.1978(8)	0.6041(10)	0.2001(6)	0.063(3)

U(eq) is 1/3 of the trace of the orthogonalized U.

diastereomers in a ratio of A : B = 55 : 45. Yield: 17 mg (0.024 mmol) of yellow crystals (70%).

Anal. Found: C, 57.85; H, 4.89; N, 1.98. $C_{32}H_{32}FeNO_3PPd$. Calc.: C, 57.22; H, 4.76; N, 2.08%.

Isomer A: ^{1}H-NMR: δ 1.40–1.70 (m, 2H), 1.95 (m, 2H), 2.26 (m, 1H), 2.52 (m, 1H), 3.00 (s, 3H, N-CH$_3$), 3.23 (s, 3H, N-CH$_3$), 3.27 (m, 1H), 3.66 (dd, J = 3.5 Hz, 10Hz, 1H, MA), 3.89 (s, 5H, Fc), 3.92 (dd, J = 2 Hz, 2.5 Hz, 1H, Fc), 4.16 (dd, J = 3.5 Hz, 3.5 Hz, 1H, MA), 4.49 (d, J = 2.5 Hz, 1H, Fc), 7.1–7.7 (m, 10H, Ph). ^{13}C-NMR: δ 20.07, 22.37, 25.18, 42.74 (N-CH$_3$), 47.52 (d, J = 2 Hz, MA), 49.82 (d, J = 30 Hz, MA), 52.18 (N-CH$_3$), 61.31 (d, J = 1.5 Hz), 66.27 (d, J = 38 Hz, Fc), 69.30, 69.79 (d, J = 4 Hz, Fc), 71.58 (Fc), 90.31 (d, J = 22 Hz, Fc), 90.55 (d, J = 8 Hz, Fc), 128-129 (m, Ph), 129.18 (d, J = 1.5 Hz, Ph), 130.70 (d, J = 2 Hz, Ph), 131.87 (d, J = 14 Hz, Ph), 132.87 (d, J = 4.5 Hz, Ph), 134.53 (d, J = 16 Hz, Ph), 136.05, 171.17 (MA), 172.75 (MA). ^{31}P-NMR: δ 16.79.

Isomer B: ^{1}H-NMR: δ 1.40–1.70 (m, 2H), 1.95 (m, 2H), 2.26 (m, 1H), 2.52 (m, 1H), 2.89 (s, 3H, N-CH$_3$), 3.27 (m, 1H), 3.30 (s, 3H, N-CH$_3$), 3.78 (dd, J = 3.5 Hz, 10 Hz, 1H, MA), 4.00 (s, 5H, Fc), 3.99 (dd, J = 2 Hz, 2.5 Hz, 1H, Fc), 4.49 (d, J = 2.5 Hz, 1H, Fc), 4.51 (dd, J = 3.5 Hz, 3.5 Hz, 1H, MA), 7.1–7.7 (m, 10H, Ph). ^{13}C-NMR: δ 20.25, 22.14, 25.33, 44.34 (N-CH$_3$), 47.92 (d, J = 2 Hz, MA), 48.96 (d, J = 31 Hz, MA), 50.31 (N-CH$_3$), 60.39 (d, J = 2 Hz), 66.90 (d, 40 Hz, Fc), 69.48, 69.73 (d, J = 4 Hz, Fc), 71.29 (Fc), 89.74 (d, J = 21 Hz, Fc), 91.50 (d, J = 8 Hz, Fc), 128-129 (m), 129.45 (d, J = 1.5 Hz, Ph), 130.63 (d, J = 2 Hz, Ph), 131.80 (d, J = 14 Hz, Ph), 132.53 (d, J = 4 Hz, Ph), 134.42 (d, J = 16 Hz, Ph), 136.62, 171.1 (MA), 172.75 (MA). ^{31}P-NMR: δ 16.04.

4.4. {[η^5-Cyclopentadienyl]-[η^5-4-(endo-dimethyl-amino)-3-(diphenylphosphino)-4,5,6,7-tetrahydro-1H-indenyl]-iron}(η^2-tetracyanoethylene)platinum(0), 6

10 mg (0.024 mmol) of (4,5-diazafluorenone)(η^2-TCNE)platinum(0) and 12 mg (0.026 mmol) of **2a** are

Table 4
Final coordinates and equivalent isotropic thermal parameters of the non-hydrogen atoms for compound **13** $C_{29}H_{33}ClFeNPPt$ (esds in parentheses)

Atom	x	y	z	U(eq) (Å^2)
Pt(1)	0.22797(2)	0.42927(2)	0.25837(1)	0.0196(1)
Fe(1)	0.28616(6)	0.83907(7)	0.30415(5)	0.0174(2)
Cl(1)	0.11307(14)	0.3087(2)	0.26939(11)	0.0421(6)
P(1)	0.34667(12)	0.53843(13)	0.26136(8)	0.0162(4)
N(1)	0.0795(4)	0.5594(4)	0.1598(3)	0.0216(12)
C(1)	0.3159(4)	0.7095(5)	0.2484(3)	0.0162(17)
C(2)	0.2021(4)	0.7533(5)	0.1887(3)	0.0186(17)
C(3)	0.2050(5)	0.8941(5)	0.1842(3)	0.0213(17)
C(4)	0.3176(5)	0.9351(5)	0.2400(3)	0.0206(17)
C(5)	0.3869(5)	0.8230(5)	0.2793(3)	0.0193(17)
C(6)	0.3856(6)	0.8257(7)	0.4295(4)	0.042(2)
C(7)	0.2845(7)	0.7609(7)	0.3896(4)	0.046(3)
C(8)	0.1967(6)	0.8531(6)	0.3404(4)	0.037(2)
C(9)	0.2446(5)	0.9750(6)	0.3493(4)	0.0272(19)
C(10)	0.3615(6)	0.9566(6)	0.4049(3)	0.033(2)
C(11)	0.1026(5)	0.6695(6)	0.1262(3)	0.0226(17)
C(12)	0.0010(5)	0.7597(7)	0.0606(4)	0.0367(19)
C(13)	0.0001(5)	0.8911(6)	0.0939(4)	0.0372(19)
C(14)	0.1001(5)	0.9740(6)	0.1262(4)	0.0312(17)
C(15)	0.4945(5)	0.5245(5)	0.3538(3)	0.0181(17)
C(16)	0.5718(5)	0.4751(6)	0.3518(4)	0.0273(19)
C(17)	0.6825(5)	0.4611(7)	0.4245(4)	0.038(2)
C(18)	0.7165(5)	0.4985(7)	0.4988(4)	0.0322(19)
C(19)	0.6408(5)	0.5471(6)	0.5020(3)	0.032(2)
C(20)	0.5297(5)	0.5601(6)	0.4297(4)	0.033(2)
C(21)	0.3379(5)	0.4981(5)	0.1748(3)	0.0199(17)
C(22)	0.3624(6)	0.5901(6)	0.1425(4)	0.037(3)
C(23)	0.3526(7)	0.5566(7)	0.0754(4)	0.047(3)
C(24)	0.3231(6)	0.4302(8)	0.0440(4)	0.043(2)
C(25)	0.3020(5)	0.3392(7)	0.0775(4)	0.0343(19)
C(26)	0.3082(5)	0.3736(6)	0.1428(3)	0.0265(17)
C(27)	0.0229(5)	0.6096(6)	0.1875(4)	0.0307(19)
C(28)	0.0028(5)	0.4629(6)	0.0914(4)	0.037(2)
C(29)	0.3505(5)	0.2942(6)	0.3374(4)	0.033(2)

U(eq) is 1/3 of the trace of the orthogonalized U.

dissolved in 3 ml CH_2Cl_2. After stirring for 3 h the complex is precipitated by addition of diethyl ether yielding 5 mg (0.006 mmol) of orange crystals (26%).

^{1}H-NMR: δ 1.43 (m, 1H), 1.71 (m, 2H), 2.02 (m, 2H), 2.40 (m, 1H), 2.66 (m, 1H), 3.55 (m, 1H), 3.59 (s, 3H, N–CH$_3$), 3.60 (s, 3H, N–CH$_3$), 3.95 (s, 5H, Fc), 4.33 (dd, $J = 2$ Hz, 2 Hz, 1H, Fc), 4.69 (d, $J = 2$ Hz, 1H, Fc), 7.1–8.0 (m, 10 H, Ph). ^{13}C-NMR: δ 21.20, 22.48, 24.55, 47.26 (N–CH$_3$), 55.58 (N–CH$_3$), 64.43 (d, $J = 2.5$ Hz), 65.33 (d, $J = 50$ Hz, Fc), 69.85 (d, $J = 2.5$ Hz), 70.88 (d, $J = 6$ Hz), 72.21 (Fc), 90.34 (d, $J = 9$ Hz, Fc), 115.00 (m, CN), 128.87 (d, $J = 12$ Hz, Ph), 129.01 (d, $J = 11$ Hz, Ph), 130.97 (d, $J = 2.5$ Hz, Ph), 131.72 (d, $J = 12$ Hz, Ph), 132.12 (d, $J = 2.5$ Hz, Ph), 133.95 (d, $J = 14$ Hz, Ph). ^{31}P-NMR: δ 12.38 ($J_{Pt-P} = 4283$ Hz).

4.5. {[η^5-Cyclopentadienyl]-[η^5-4-(endo-dimethyl-amino)-3-(diphenylphosphino)-4,5,6,7-tetrahydro-1H-indenyl]-iron}(η^2-maleic anhydride)platinum(0), 7

The synthesis of 7 was carried out in a manner similar to that of 4. Yield: 13 mg (0.017 mmol) of orange crystals (50%).

^{1}H-NMR: δ 1.67 (m, 1H), 2.02 (m, 2H), 2.32 (m, 1H), 2.53 (m, 1H), 3.12 (s, 3H, N–CH$_3$), 3.49 (m, 1H, MA), 3.49 (m, 1H), 3.54 (s, 3H, N–CH$_3$), 3.93 (s, 5H, Fc), 4.03 (dd, $J = 2$ Hz, 2 Hz, 1H, Fc), 4.12 (m, 1H,

MA), 4.57 (d, $J = 2$ Hz, 1H, Fc), 7.1–7.7 (m, 10H, Ph). ^{31}P-NMR: δ 17.68 ($J_{Pt-P} = 4478$ Hz).

4.6. {[η^5-Cyclopentadienyl]-[η^5-4-(endo-N,N-dimethyl-amino)-3-(diphenylphosphino)-4,5,6,7-tetrahydro-1H-indenyl]-iron}dichloropalladium(II), 8

A suspension of 110 mg (0.42 mmol) dichloro(bi-sacetonitrilo)palladium(II) in 8 ml degassed benzene is treated under argon with a solution of 200 mg (0.43 mmol) of 2a in 5 ml benzene. After stirring for 3 h 8 precipitates and is filtered off and washed with benzene and ether. The crude product can be recrystallized from CHCl$_3$–hexane. Yield: 260 mg (0.40 mmol) of dark red crystals (95%); decomp: 205°C. Anal. Found: C, 50.6; H, 4.89; N, 1.97. C$_{28}$H$_{30}$Cl$_2$FeNPPd xH$_2$O. Calc.: C, 50.76; H, 4.83; N, 2.11%.

^{1}H-NMR: δ 1.62 (m, 2H), 1.95 (m, 1H), 2.05 (m, 1H), 2.28 (ddd, $J = 8$ Hz, 5.5 Hz, 16 Hz, 1H), 2.55 (ddd, $J = 7$ Hz, 5 Hz, 16 Hz, 1H), 3.13 (dd, $J = 6.5$ Hz, 6.5 Hz, 1H), 3.20 (s, 3H, N–CH$_3$), 3.47 (s, 3H, N–CH$_3$), 3.82 (dd, $J = 2.5$ Hz, 2.5 Hz, 1H, Fc), 4.28 (s, 5H, fc), 4.61 (d, $J = 2.5$ Hz, 1H, Fc), 7.38–7.76 (m, 10H, Ph). ^{13}C-NMR: δ 21.9, 22.8, 25.0, 42.9 (N–CH$_3$), 51.6 (N–CH$_3$), 62.5 (d, $J = 3.8$ Hz), 70.1 (Fc), 71.3 (d, $J = 5$ Hz, Fc), 72.4 (5C, Fc), 89.0 (Fc), 90.8 (Fc), 92.8 (Fc), 127.9 (d, $J = 12.2$ Hz, Ph), 129.0 (d, $J = 8$ Hz, Ph) 129.2 (d, $J = 11$ Hz, Ph), 129.6 (d, $J = 31$ Hz, Ph),

Table 5
Selected bond lengths (Å) and bond angles (deg) for 4, 6, 8 [4] and 13

	4	6	8	13
Tilt angle Cp^1/Cp^2 [a]	7.1(4)	6.3(4)	9.5(3)	8.9(5)
Selected bond lengths				
Pd/Pt–N1	2.246(4)	2.158(5)	2.171(4)	2.275(5)
Pd/Pt–P1	2.271(2)	2.233(1)	2.207(2)	2.175(1)
Pd/Pt–X [b]	C30: 2.022(7)	C30: 2.034(6)	Cl2: 2.282(3)	C29: 2.044(6)
Pd/Pt–Y [c]	C29: 2.112(6)	C29: 2.145(5)	Cl1: 2.376(3)	Cl1: 2.363(2)
Selected bond angles				
N1–Pd/Pt–P1	94.32(12)	97.61(12)	95.22(12)	94.61(12)
X–Pd/Pt–Y [c]	41.2(2)	42.8(2)	89.09(8)	87.0(2)
Distances from Cp^1-plane [d]				
C11	–0.298(6)	–0.281(6)	–0.325(5)	–0.338(7)
C12	–0.637(7)	0.011(7)	–0.547(5)	–0.562(8)
C13	0.150(7)	–0.682(7)	0.286(5)	0.286(8)
C14	–0.121(7)	–0.037(6)	–0.029(5)	–0.039(8)
N1	0.705(5)	0.358(5)	0.587(3)	0.543(6)
C27	1.840 [e]	1.788 [e]	1.852 [e]	1.813 [e]
C28	0.006(6)	–0.369(10)	–0.110(5)	–0.181(8)
P1	0.073(3)	–0.135(1)	–0.184(1)	–0.210(2)
Pd/Pt	1.551 [e]	0.355(1)	1.011(1)	0.929(1)
X	2.807 [e]	0.475(6)	1.155(1)	1.173(8)
Y	3.124 [e]	0.879(6)	2.477 [e]	2.324 [e]

[a] Cp^1, Cp^2: least squares planes defined by carbons C1–C5 (Cp^1) and C6–C10 (Cp^2). [b] X: substituent in trans position to N1 (see Scheme 1). [c] Y: substituent in trans position to P1 (see Scheme 1). [d] Positive values indicate atom displacement towards the proximal Cp^1 side (the iron coordinated Cp side), negative values indicate atom displacements towards the distal Cp^1 side. [e] No esd calculated.

131.4 (d, *J* = 3 Hz, Ph), 131.7 (d, *J* = 3 Hz, Ph), 133.3 (d, *J* = 11 Hz, Ph), 134.5 (d, *J* = 11 Hz, Ph). ^{31}P-NMR (CDCl$_3$): δ 15.85.

4.7. {[η^5-Cyclopentadienyl]-[η^5-4-(endo-N,N-dimethyl-amino)-3-(diphenylphosphino)-4,5,6,7-tetrahydro-1H-indenyl]-iron}(chloro)methylpalladium(II), 9

To 26 mg (0.1 mmol) of (COD)Pd(Me)Cl dissolved in 5 ml degasssed absolute CH$_2$CL$_2$ a solution of 50 mg (0.107 mmol) of **2a** in CH$_2$Cl$_2$ is added. After stirring for 1 h the solvent is removed in vacuo, the precipitate dissolved in 1 ml CH$_2$Cl$_2$ and filtered off celite. The product is precipitated by addition of hexane. Yield: 60 mg (0.095 mmol) of yellow crystals (95%).Anal. Found: C, 55.11; H, 5.00; N, 2.18. C$_{29}$H$_{33}$ClFeNPPd. Calc.: C, 55.81; H, 5.29; N, 2.25%.

^{1}H-NMR: δ 0.88 (d, *J* = 3 Hz, 3H, Pd–C*H*$_3$), 1.59 (m, 2H), 2.00 (m, 2H), 2.25 (ddd, *J* = 6 Hz, 6 Hz, 16 Hz, 1H), 2.54 (ddd, *J* = 6 Hz, 6 Hz, 16 Hz, 1H), 2.87(s, 3H, N–CH$_3$), 3.07 (dd, *J* = 6 Hz, 6 Hz, 1H), 3.19 (s, 3H, N–CH$_3$), 3.74 (dd, *J* = 2 Hz, 2 Hz, 1H, Fc), 4.18 (s, 5H, Fc), 4.49 (d, *J* = 2 Hz, 1H, Fc), 7.1–7.6 (m, 15H, Ph). ^{13}C-NMR: δ −0.04(d, J_{P-C} = 2.5 Hz, Pd–CH$_3$), 21.32, 23.19, 25.86, 40.03 (N–*C*H$_3$), 48.67 (N–CH$_3$), 60.68, 66.40 (d, *J* = 54 Hz), 69.76, 70.24 (d, *J* = 5 Hz), 72.31 (Fc), 90.26 (d, *J* = 19 Hz, Fc), 91.85 (d, *J* = 10 Hz, Fc), 128.60 (d, *J* = 10 Hz, Ph), 129.18 (d, *J* = 10 Hz, Ph), 130.50 (Ph), 131.50 (m, Ph), 132.30, 132.80, 133.55 (d, *J* = 12 Hz, Ph), 134.51 (d, *J* = 10 Hz, Ph). ^{31}P-NMR: δ 27.05.

4.8. {[η^5-Cyclopentadienyl]-[η^5-4-(endo-dimethyl-amino)-3-(diphenylphosphino)-4,5,6,7-tetrahydro-1H-indenyl]-iron}(iodo)phenylpalladium(II), 10.

Method A: to a degassed solution of 43 mg (0.1 mmol) (tmeda)Pd(C$_6$H$_5$)I in 2 ml CH$_2$Cl$_2$ a solution of 51 mg (1.1 mmol) of **2a** in 5 ml CH$_2$Cl$_2$ is added under argon. The reaction mixture is stirred at room temperature for 16 h. The reaction mixture is filtered off celite, and the solvent is evaporated in vacuo to a volume of ca. 1 ml. The crude complex is precipitated by addition of pentane. Crystallization from CHCl$_3$–hexane gave 70 mg (0.09 mmol) of pale red crystals (90%). Crystals suitable for X-ray analysis were obtained from CH$_2$Cl$_2$–hexane at 4°C.

Method B: to a degassed solution of Pd$_2$(dba)$_3$-(CHCl$_3$) (100 mg, 0.097 mmol) in toluene (20 ml) are added 100.5 mg (0.232 mmol) of **2a** and 98.5 mg (0.483 mmol) of PhI. The reaction mixture is stirred for 16 h, the orange-red precipitate is filtered off and washed with hexane. Yield: 65 mg (43%). Anal. Found: C, 52.50; H, 4.63; N, 1.61. C$_{34}$H$_{35}$FeINPPd. Calc.: C, 52.22; H, 4.50; N, 1.80%.

^{1}H-NMR: δ 1.40 (m, 1H), 1.68 (m, 1H), 1.95 (m, 1H), 2.06 (m, 1H), 2.23 (ddd, *J* = 4.5 Hz, 10 Hz, 15

Hz, 1H), 2.56 (ddd, *J* = 5 Hz, 5 Hz, 15 Hz, 1H), 3.03 (m, 1H), 3.06 (s, 3H, N–CH$_3$), 3.35 (s, 3H, N–CH$_3$), 4.20 (s, 1H, Fc), 4.35 (s, 5H, Fc), 4.53 (d, *J* = 2 Hz, 1H, Fc), 6.4–6.6 (m, 3H, Ph), 6.9–7.5 (m, 12H, Ph). ^{13}C-NMR: δ 21.36, 22.63, 25.52, 60.25 (d, *J* = 2 Hz), 43.10 (N–CH$_3$), 50.08 (N–*C*H$_3$), 66.81 (d, *J* = 48 Hz), 69.64, 72.53 (Fc), 90.36 (d, *J* = 19 Hz, Fc), 91.59 (d, *J* = 8 Hz, Fc), 122.34 (Ph), 127.32 (Ph), 128.16 (d, *J* = 10.5 Hz, Ph), 128.99 (d, *J* = 10 Hz, Ph), 130.08 (d, *J* = 43 Hz, Ph), 130.21 (Ph), 131.06 (Ph), 132.60 (d, *J* = 45 Hz, Ph), 133.47 (d, *J* = 10.5 Hz, Ph), 134.30 (d, *J* = 12 Hz, Ph). ^{31}P-NMR: δ 17.46.

4.9. {[η^5-Cyclopentadienyl]-[η^5-4-(endo-dimethyl-amino)-3-(diphenylphosphino)-4,5,6,7-tetrahydro-1H-indenyl]-iron}(bromo)benzylpalladium(II), 11

To 22 mg (0.05 mmol) of (bipy)Pd(Bz)Br dissolved in 3 ml CH$_2$Cl$_2$ a solution of 26 mg (0.055 mmol) of **2a** in CH$_2$Cl$_2$ is added under argon. The reaction mixture is stirred for 6 h, filtered off celite and the solvent is removed in vacuo. The precipitate is dissolved in 1 ml CH$_2$Cl$_2$ and crystallized by addition of diethyl ether. Yield: 34 mg (0.045 mmol) of orange crystals (90%).

^{1}H-NMR: δ 1.17 (m, 1H), 1.61 (m, 1H), 1.86 (m, 1H), 1.97 (m, 1H), 2.14 (ddd, *J* = 5.5 Hz, 10 Hz, 15 Hz, 1H), 2.47 (ddd, *J* = 5 Hz, 5 Hz, 15 Hz, 1H), 2.75 (s, 3H, N–C*H*$_3$), 2.75 (m, 2H), 3.22 (s, 3H, (N–C*H*$_3$), 3.89 (dd, *J* = 2 Hz, 2 Hz, 1H, Fc), 4.26 (s, 5H, Fc), 4.36 (m, 1H), 4.43 (d, *J* = 2 Hz, 1H, Fc), 6.8–7.7 (m, 15H, Ph). ^{13}C-NMR: δ 21.17, 22.48, 25.56, 41.37 (N–*C*H$_3$), 48.89 (N–CH$_3$), 59.11, 67.69 (d, *J* = 54 Hz), 69.16 (d, *J* = 4 Hz), 69.41, 72.41 (Fc), 89.94 (d, *J* = 18 Hz), 91.97 (d, *J* = 8 Hz), 124.67, 128.17, 128.85 (d, *J* = 10.5 Hz), 128.98 (d, *J* = 9 Hz), 129.60, 130.60, 131.21 (d, *J* = 14 Hz), 131.80 (d, *J* = 42 Hz), 134.50 (m), 146.14. ^{31}P-NMR: δ 23.25.

4.10. {[η^5-Cyclopentadienyl]-[η^5-4-(endo-dimethyl-amino)-3-(diphenylphosphino)-4,5,6,7-tetrahydro-1H-indenyl]-iron}dichloroplatinum(II), 12

To a degassed solution of 46.7 mg (0.1 mmol) of **2a** in 4 ml CH$_2$Cl$_2$ a degassed solution of 35.5 mg (0.095 mmol) of (COD)PtCl$_2$ in CH$_2$Cl$_2$ is added. After stirring for 30 min the volume of the solvent is reduced in vacuo to ca. 2 ml, the complex is precipitated by addition of pentane. The yellow microcrystals were recrystallized from CH$_2$Cl$_2$–pentane, yielding 68 mg (0.093 mmol) of yellow-orange crystals (98%).

^{1}H-NMR: δ 1.67 (m, 2H), 1.95 (m, 1H), 2.11 (m, 1H), 2.31 (ddd, *J* = 7 Hz, 7 Hz, 16 Hz, 1H), 2.57 (ddd, *J* = 5 Hz, 5 Hz, 16 Hz, 1H), 3.35 (dd, *J* = 6 Hz, 6 Hz, 1H), 3.43 (s, 3H, N–C*H*$_3$), 3.68 (s, 3H, N–C*H*$_3$), 3.85 (dd, *J* = 2 Hz, 2 Hz, 1H, Fc), 4.22 (s, 5H, Fc), 4.59 (d,

$J = 2$ Hz, 1H Fc), 7.3–7.8 (m, 10H, Ph). ^{13}C-NMR: δ 22.41, 22.56, 24.85, 43.61 (N–CH_3), 52.88 (N–CH_3), 62.45 (d, $J = 71$ Hz, Fc), 64.18 (d, $J = 3.5$ Hz), 69.51 (d, $J = 3.5$ Hz), 70.36 (d, $J = 6$ Hz), 71.98 (Fc), 87.81 (d, $J = 17$ Hz, Fc), 91.99 (d, $J = 9$ Hz, Fc), 127.29 (d, $J = 12$ Hz, Ph), 128.58 (d, $J = 11$ Hz, Ph), 130.80 (d, $J = 2.5$ Hz, Ph), 130.92 (d, $J = 2.5$ Hz, Ph), 132.55 (d, $J = 11$ Hz, Ph), 134.15 (d, $J = 11$ Hz, Ph). ^{31}P-NMR: δ – 10.12 ($J_{P–P} = 3979$ Hz).

4.11. {[η^5-Cyclopentadienyl]-[η^5-4-(endo-dimethyl-amino)-3-(diphenylphosphino)-4,5,6,7-tetrahydro-1H-indenyl]-iron}(chloro)methylplatinum(II), 13

A solution of 53 mg (0.11 mmol) of **2a** and 35.3 mg (0.1 mmol) of (COD)Pt(CH_3)Cl in 20 ml dry degassed dichloromethane is stirred for 4 h at room temperature. After reducing the solvent to ca. 2 ml the complex is precipitated by addition of pentane. Crystals suitable for X-ray analysis were obtained by crystallization from CH_2Cl_2–hexane. Yield: 68 mg (0.095 mmol) of pale orange crystals (95%).

^{1}H-NMR: δ 0.77 (d, $J_{P–H} = 3.5$ Hz, 3H, Pt–CH_3), 1.60 (m, 2H), 1.95 (m, 1H), 2.05 (m, 1H), 2.27 (ddd, $J = 5$ Hz, 6 Hz, 16 Hz, 1H), 2.55 (ddd, $J = 6$ Hz, 8 Hz, 16 Hz, 1H), 3.04 (s, 3H, N–CH_3), 3.26 (dd, $J = 6$ Hz, 6 Hz, 1H), 3.34 (s, 3H, N–CH_3), 3.76 (dd, $J = 2$ Hz, 2 Hz, 1H, Fc), 4.15 (s, 5H, Fc), 4.49 (d, $J = 2$ Hz, 1H, Fc), 7.3–7.7 (m, 10H, Ph). ^{13}C-NMR: δ – 17.95 (d, $J_{P–C} = 7$ Hz, Pt–CH_3, $J_{P–C} = 609$ Hz), 22.04, 23.35, 25.85, 40.62 (N–CH_3), 49.53 (N–CH_3), 61.93 (d, $J = 1.5$ Hz), 66.48 (d, $J = 68$ Hz, Fc), 69.74 (d, $J = 3$ Hz, Fc), 70.08 (d, $J = 6$ Hz, Fc), 72.37 (Fc), 89.88 (d, $J = 16$ Hz, Fc), 91.57 (d, $J = 9$ Hz, Fc), 128.21 (d, $J = 12$ Hz, Ph), 128.88 (d, $J = 12$ Hz, Ph), 129.30 (d, $J = 68$ Hz, Ph), 130.90 (Ph), 131.20 (Ph), 131.70 (d, $J = 60$ Hz, Ph), 133.20 (d, $J = 10.5$ Hz, Ph), 134.59 (d, $J = 10.5$ Hz, Ph). ^{31}P-NMR (CDCl$_3$): δ 5.81 ($J_{Pt–P} = 4902$ Hz).

4.12. X-ray structure determination of 4, 6 and 13

Crystal data and details on data collection and refinement are presented in Table 1. Final atomic coordinates and equivalent isotropic thermal parameters for compounds **4**, **6**, and **13** are listed in Tables 2, 3, and 4.

Crystals suitable for X-ray structure determination were cut to size and mounted on a Lindemann-glass capillary, and subsequently transferred into the cold nitrogen stream on an Enraf–Nonius CAD4-T diffractometer on rotating anode. Accurate unit-cell parameters and an orientation matrix were determined from the setting angles of 25 reflections (SET 4) [30] (20 reflections for **4**). The unit-cell parameters were checked for the presence of higher lattice symmetry [31]. For compound **13** the monoclinic unit cell can be transformed to

a metrically orthorhombic unit cell. However, orthorhombic Laue symmetry is not supported by the reflection data: R(av) ~ 50%. Data were collected at 150 K in $\omega/2\theta$ scan mode with scan angle $\Delta\omega = \alpha +$ 0.35 tan $\theta°$, where α is 0.66, 0.91 and 0.80 for **4**, **6** and **13**, respectively. Data were corrected for Lp effects, and for linear decay of the three periodically measured reference reflections. An empirical absorption/extinction correction was applied (DIFABS [32] as implemented in PLATON [33]). The structures were solved by automatic Patterson methods and subsequent difference Fourier techniques DIRDIF-92 [29]. Refinement on F^2 was carried out by full-matrix least square techniques (SHELXL-93) [34]); no observance criterion was applied during refinement. All non-hydrogen atoms were refined with anisotropic thermal parameters. The hydrogen atoms were refined with a fixed isotropic thermal parameter amounting to 1.5 for the methyl hydrogen atoms or 1.2 for the other hydrogen atoms times the value of the equivalent isotropic thermal parameter of their carrier atoms. The hydrogen atoms on C29 and C30 of **4** were refined without any geometrical restraints and its thermal parameter fixed at 1.5 times the value of the equivalent isotropic thermal parameter of the carrier atom. Weights were optimized in the final refinement cycles. The structure of **4** has two voids of approximately 250 Å^3, each yielding an electron count of 84 electrons, amounting to two dichloromethane molecules per void, four per unit cell (PLATON / SQUEEZE [35]). The structure of **13** contains small voids (less than 9 Å^3, near C 13); however, no significant residual density was found in that area (PLATON / SQUEEZE [35]). Neutral atom scattering factors and anomalous dispersion corrections were taken from *International Tables for Crystallography* [36].

Geometric calculations and illustrations were performed with PLATON [33]; all calculations were performed on a DEC5000/125. Further details of the crystal structure investigation may be obtained from one of the authors (A.L.S.).

Acknowledgements

References

[1] A. Togni and T. Hayashi (eds.), Ferrocenes, VCH, Weinheim, 1995.

[2] T. Hayashi, in I. Ojima (ed.), Catalytic Asymmetric Synthesis, VCH, Weinheim, 1993, p. 323.

[3] A. Togni, C. Breutel, A. Schnyder, F. Spindler, H. Landert and A. Tijani, J. Am. Chem. Soc., 116 (1994) 4062.

[4] B. Jedlicka, Ch. Kratky, W. Weissensteiner and M. Widhalm, J. Chem. Soc. Chem. Commun., (1993) 1329.

[5] H. Wally, Ch. Kratky, W. Weissensteiner, M. Widhalm and K. Schlögl, J. Organomet. Chem., 450 (1993) 185.

[6] H. Wally, K. Schlögl, W. Weissensteiner and M. Widhalm, Tetrahedron Asymm., 4 (1993) 285.

[7] A. Mernyi, Ch. Kratky, W. Weissensteiner and M. Widhalm, J. Organomet. Chem., in press.

[8] G. Kutschera, Ch. Kratky, W. Weissensteiner and M. Widhalm, J. Organomet. Chem., in press.

[9] T. Hayashi, M. Konishi, M. Fukushima, T. Mise, M. Kagotani, M. Tajika and M. Kumada, J. Am. Chem. Soc., 104 (1982) 180.

[10] R. Fernández-Gelán, F.A. Jalón, B.R. Manzano, J. Rodríguez-de la Fuente, M. Vrahami, B. Jedlicka, Ch. Kratky and W. Weissensteiner, in preparation.

[11] T. Hayashi, M. Konishi and M. Kumada, Tetrahedron Lett., 21 (1979) 1871.

[12] J.M. Brown, N.A. Cooley and D.W. Price, J. Chem. Soc., Chem. Commun., (1989) 458.

[13] K.V. Baker, J.M. Brown, N.A. Cooley, G.D. Hughes and R.J. Taylor, J. Organomet. Chem., 370 (1989) 397.

[14] T. Ukai, H. Kawazura, Y. Ishii, J.J. Bonnet and J.A. Ibers, J. Organomet. Chem., 65 (1974) 253.

[15] R.A. Klein and C.J. Elsevier, IXth ISHC, Jerusalem, 1994.

[16] P.W.N.M. van Leeuwen and C.F. Roobeek, Eur. Patent Appl. 380162, 1990.

[17] (a) G. Yoshida, S. Numata and H. Kurosawa, Chem. Lett., (1976) 705; (b) H. Kurosawa and G. Yoshida, J. Organomet. Chem., 120 (1976) 297.

[18] B.A. Markies, A.J. Canty, W. de Graaf, J. Boersma, M.D. Janssen, M.P. Hogerheide, W.J.J. Smeets, A.L. Spek and G. van Koten, J. Organomet. Chem., 482 (1994) 191.

[19] B.A. Markies, P. Wijkens, J. Boersma, H. Kooijman, N. Veldman, A.L. Spek and G. van Koten, Organometallics, 13 (1994) 3244.

[20] S. Cenini, R. Ugo and G. La Monica, J. Chem. Soc. A, (1971) 409.

[21] S. Otsuka, T. Yoshida and Y. Ishii, J. Am. Chem. Soc., 93 (1971) 6462.

[22] T. Ito, S. Hasegawa, Y. Takahashi and Y. Ishii, J. Organomet. Chem., 73 (1974) 401.

[23] K. Itoh, F. Ueda, K. Hirai and Y. Ishii, Chem. Lett., (1977) 877.

[24] M.T. Chicote, M. Green, J.L. Spencer, F.G.A. Stone and J. Vicente, J. Chem. Soc. Dalton Trans., (1979) 536.

[25] K.J. Cavell, D.J. Stufkens and K. Vrieze, Inorg. Chim. Acta, 47 (1980) 67.

[26] R. van Asselt, C.J. Elsevier, W.J.J. Smeets and A.L. Spek, Inorg. Chem., 33 (1994) 1521.

[27] R.G. Pearson, Inorg. Chem., 12 (1973) 712.

[28] J.A. Casares, S. Coco, P. Espinet and Y.-S. Lin, Organometallics, 14 (1995) 3058.

[29] P.T. Beurskens, G. Admiraal, G. Beurskens, W.P. Bosman, S. Garciá-Granda, R.O. Gould, J.M.M. Smits and C. Smykalla, Technical Rep. The DIRDIF program system, 1992 (Crystallography Laboratory, University of Nijmegen, Netherlands).

[30] J.L. de Boer and A.J.M. Duisenberg, Acta Crystallogr. Sect. A, 40 (1984) C410.

[31] A.L. Spek, J. Appl. Crystallogr., 21 (1988) 578.

[32] N. Walker and D. Stuart, Acta Crystallogr. Sect. A, 39 (1983) 158.

[33] A.L. Spek, Acta Crystallogr. Sect. A, 46 (1990) C34.

[34] G.M. Sheldrick, SHELXL-93, Program for crystal structure refinement, University of Göttingen, Germany, 1993.

[35] A.L. Spek, A.C.A. Abstr., 22 (1994) 66.

[36] A.J.C. Wilson (ed.), International Tables for Crystallography, Vol. C, Kluwer, Dordrecht, 1992.